New Poly(carbosilane) Models. 5. Pyrolysis of a Series of Functional Poly(carbosilanes)

E. Bouillon, R. Pailler, and R. Naslain*

Laboratoire des Composites Thermostructuraux, UMR-47 CNRS-SEP-UB1, Europarc, 3, Av. Léonard de Vinci, F-33600 Pessac, France

E. Bacqué, J.-P. Pillot, M. Birot, and J. Dunoguès

Laboratoire de Chimie Organique et Organométallique, UA 35-CNRS, Université Bordeaux-I, 351, Cours de la Libération, F-33405 Talence, France

P. V. Huong

Laboratoire de Spectroscopie Moléculaire et Cristalline, UA 124-CNRS, Université Bordeaux-I, 351, Cours de la Libération, F-33405 Talence, France

Received February 21, 1990. Revised Manuscript Received December 21, 1990

Ten models of functional poly(carbosilane) (PCS) or poly(carbosilazane) (PCSZ) precursors, prepared from chlorinated poly[(dimethylsilylene)methylene], were pyrolyzed, under inert gas flow or vacuum at temperatures up to 2300 °C, to derive relations between the nature of the precursors and that of the ceramic residues. The organometallic/inorganic transition and the recrystallization of the pyrolytic residues were studied by different analytical techniques. Linear precursors resulted in low ceramic yields unless a cross-linking treatment was applied prior to pyrolysis. High C content precursors do not necessarily lead to high C content ceramics. Ternary (Si–C–O or Si–C–N) and even quaternary tetrahedral species were present in the ceramic residues. Nitrogen was found to inhibit the crystallization of the ex-PCSZ ceramics up to ~1400 °C. Only part of the initial skeleton of the precursors was maintained in the ceramics.

Introduction

Ceramic materials are now commonly obtained either as powders, fibers, or fibrous composites through the pyrolysis of organic or organometallic precursors. Carbon fibers (derived from rayon, poly(acrylonitrile), or pitch) can be considered as one of the first applications of the organic precursor route to the synthesis of advanced ceramics.[1-9] More recently, ceramic matrix composites (CMC), made of ceramic fibers embedded in a ceramic matrix (based on C, SiC, Si_3N_4, B_4C, or BN), have been obtained according to a general procedure involving (i) impregnation of a fiber preform with the liquid precursors, (ii) cross-linking, and (iii) pyrolysis at moderate temperatures.[10-22]

The synthesis of SiC-based fiber from a poly(carbosilane) (PCS) precursor, by Yajima and co-workers in the mid-1970s, is an important milestone. These fibers, now produced by Nippon Carbon Co. Ltd (trademark Nicalon), are obtained according to a spinning–stabilization–pyrolysis process very similar to that previously used for carbon fibers.[23-33] They are made of silicon carbide, free carbon, and silicon oxycarbide mixed together at a nanometer scale. The fibers exhibit high tensile strength and stiffness as well as good resistance to oxidation up to about 1100 °C. Above this limit, a decrease in the mechanical properties occurs that seems to be related to a change in the microstructure of the material.[34-41] It is generally accepted

(1) Donnet, J. B., Bansal, R. C., Eds.; *Carbon Fibers*; Marcel Dekker: New York, 1985.
(2) Delmonte, J. in *Technology of Carbon Graphite Fibers Composites*; Van Nostrand Reinhold: New York, 1981; Chapter 2, pp 41–87.
(3) Goodhew, P. J.; Clarke, A. J.; Bailey, J. E. *Mater. Sci. Eng.* **1985**, *17*, 3–30.
(4) Rose, P. J. In *Processing and uses of Carbon Fibre Reinforced Plastics*; VDI Verlag: Dusseldorf, 1981; pp 5–39.
(5) Barr, J. B.; Chwastiack, S.; Didchenko, R.; Lewis, I. C.; Lewis, R. T.; Singer, L. C. *Appl. Polym. Symp.* **1976**, *29*, 161–73.
(6) (a) Singer, L. S. *Carbon* **1978**, *16*, 409–15. (b) Singer, L. S. *Fuel* **1981**, *60*, 839–47.
(7) Lewis, I. C. *J. Chim. Phys.* **1984**, *81*, 751–8.
(8) Otami, S. *Mol. Cryst. Liq. Cryst.* **1981**, *63*, 249–64.
(9) Singer, L. S. U.S. Patent 4,005,183, Jan 25, 1977.
(10) Fitzer, E.; Fritz, W.; Gadow, R. *Advanced Ceramic Materials*; Tokyo Institute Technology: Yokohama, 1983.
(11) West, R.; David, L. D.; Djurovich, P. I.; Yo, H.; Sinclair, R. *Ceram. Bull.* **1983**, *62/8*, 916–23.
(12) Yajima, S. *Ceram. Bull.* **1983**, *62/8*, 893–915.
(13) Rice, R. C. *Ceram. Bull.* **1983**, *62/8*, 889–92.
(14) Jamet, J.; Spann, J. R.; Rice, R. W.; Lewis, D.; Goblenz, W. S. 8th Annual Conference on Composites and Advanced Ceramics, Materials; Jan, 1984, Cocoa Beach, FL; pp 677–94.
(15) Wills, R. R.; Mackle, R. A.; Makhajee, S. P. *Ceram. Bull.* **1983**, *62/8*, 904–5.
(16) Walker, B. E.; Rice, R. W.; Becher, P. F.; Bender, B. A.; Goblenz, W. S. *Ceram. Bull.* **1983**, *62/8*, 916–23.
(17) Fitzer, E. *Act. Symp. Int., Factors in Densification and Sintering of Oxide or Non-oxide Ceramics*; Hakone, Japan, 1978; pp 618–73.
(18) Fitzer, E.; Schlichting, J. *High Temp. Sci.* **1980**, 149–72.
(19) Schilling, C. L.; Wesson, J. P.; Williams, T. C. *Ceram. Bull.* **1983**, *62/8*, 912–5.
(20) Hasegawa, Y.; Okamura, K. *J. Mater. Sci.* **1983**, *18*, 3633–48.
(21) Penn, B. J.; Ledbetter, F. E.; Clemous, J. H.; Daniles, J. G. *J. Appl. Polym. Sci.*, **1982**, *217*, 3751–61.
(22) Bender, B. A.; Rice, R. W.; Spann, J. R. *Com. Am. Ceram. Soc.* **1987**, *70*, C58–C60.
(23) Yajima, S.; Hasegawa, Y.; Hayashi, J.; Iimura, M. *J. Mater. Sci.* **1973**, *13*, 2529–76.
(24) Hasegawa, Y.; Okamura, K. *J. Mater. Sci.* **1963**, *18*, 3633–48.
(25) Hasegawa, Y.; Imura, M.; Yajima, S. *J. Mater. Sci.* **1980**, *15*, 720–8.
(26) Okamura, K.; Sato, M.; Hasegawa, Y. *J. Mat. Sci. Lett.* **1983**, *2*, 769–71.
(27) Yajima, S.; Okamura, K.; Hayashi, J.; Omon, M. *J. Am. Ceram. Sci.* **1976**, *59*, 324–77.
(28) Ichikawa, H.; Machino, F.; Mitsuno, S.; Ichikawa, T.; Okamura, K.; Hasegawa, Y. *J. Mater. Sci.* **1986**, *21*, 4352–8.
(29) Ichikawa, H.; Teranishi, H.; Ichikawa, T. *J. Mater. Sci. Lett.* **1987**, *6*, 420–2.
(30) Okamura, K.; Matsuzawa, T.; Hasegawa, Y. *J. Mater. Sci. Lett.* **1985**, *4*, 55–7.
(31) Yajima, S.; Okamura, K.; Hayashi, J. *Chem. Lett.* **1975**, 1209–12.
(32) Yajima, S.; Hayashi, J.; Omori, M. *Chem. Lett.* **1975**, 931–4.
(33) Okamura, K.; Sato, M.; Mattsuzawa, T. *Polym. Prepr. (Am. Chem. Soc., Div. Polym. Chem.)* **1984**, *25*, 6–7.

0897-4756/91/2803-0356$02.50/0

Table I. Synthesis and Identification of the Model Functional PCS and PCSZ Precursors[a]

reactants	solvt	theoret formula	ref[a]
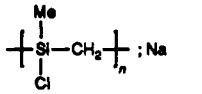	xylene	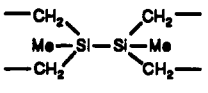	(Na, s) Si-Si (Na, i)
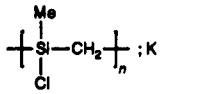	THF	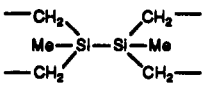	(K, s) Si-Si (K, i)
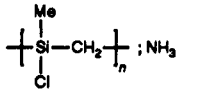	CH_2Cl_2	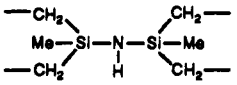	SiNHSi
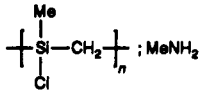	CH_2Cl_2	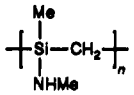	SiNHMe
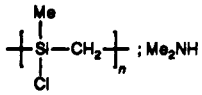	CH_2Cl_2	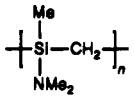	$SiNMe_2$
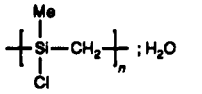	none	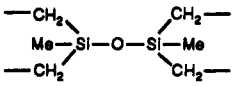	SiOSi
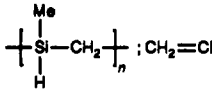	none	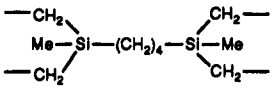	SiC_4Si
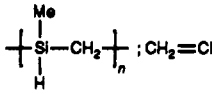	none	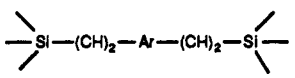	SiC_2ArC_2Si

[a] S and i refer respectively to the soluble and insoluble fraction in said solvent.

that evolution of gaseous oxygen-containing species (i.e., SiO and CO)[42,43] takes place above 1200 °C with simultaneously a coarsening of the silicon carbide grains and formation (or rearrangement) of free carbon at the grain boundaries.[44-52] However, the complexity of the material has up to now precluded a detailed understanding of the behavior of the fibers as well as an improvement of their mechanical characteristics at high temperatures. It is anticipated that free carbon and combined oxygen may play an important role.

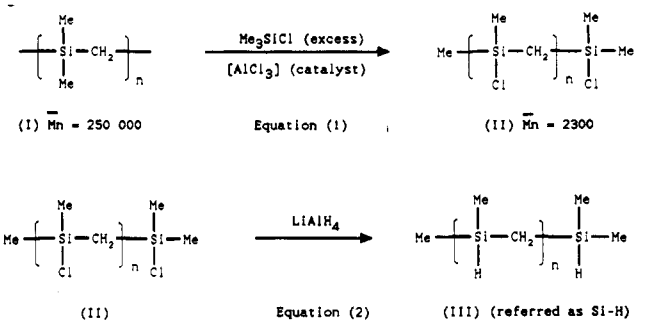

Figure 1. Important intermediates in the synthesis of the PCS or PCSZ model precursors.

To overcome the drawbacks of the ex-PCS SiC-based fibers, approaches based on the use of polysilazane (PSZ) or poly(carbosilazane) (PCSZ) precursors to prepare Si-C-N (or Si-C-N-O) fibers and even poly(titanosiloxane) precursors for Si-C-Ti-O fibers have been explored.[53-58] Concurrently, Okamura et al. have shown that Si-N-O

(34) Simon, G.; Bunsell, A. R. *J. Mater. Sci.* **1984**, *19*, 3649-57.
(35) Simon, G.; Bunsell, A. R. *J. Mater. Sci. Lett.* **1983**, *2*, 80-2.
(36) Yajima, S.; Okamura, K.; Matsuzawa, T.; Schishido, T. *Nature* **1979**, *279*, 311-3.
(37) Guimon, M. *Rev. Phys. Appl.* **1988**, *23*, 229-38.
(38) Maniette, Y.; Oberlin, A., *Mater. Sci.*, in press.
(39) Laffon, C.; Flank, A. M.; Hagege, R.; Olry, P.; Cotteret, J.; Dixmier, S.; Laridjani, M.; Legrand, A. P.; Hommel, B. *J. Mater. Sci.*, in press.
(40) Pysher, O. J.; Goretta, K. C.; Hodder, R. S.; Tressler, R. E. Presented at the 89th Annual Meeting of the American Ceramic Society; Pittsburgh, PA, Apr 29, 1987; No. 145-C-87.
(41) Chaim, R.; Hewer, A. H.; Chen, R. T. *J. Am. Ceram. Soc.* **1988**, *71*, 960-9.
(42) Johnson, S. M.; Brittain, R. D.; Lamoreaux, R. H.; Rowcliffe, D. J. *J. Am. Ceram. Soc.* **1988**, *71*, C132-C135.
(43) Luthra, K. L. *J. Am. Ceram. Soc.* **1986**, *69*, C231-C233.
(44) Fitzer, E.; Gadow, R. *Am. Ceram. Soc. Bull.* **1986**, *65*, 326-35.
(45) Hamminga, R.; Grathwolth, G.; Thummler, F. *J. Mater. Sci.* **1983**, *18*, 353-64.
(46) Fukunaga, H.; Goda, K. *Progress in Advanced Materials and Processes*; Elsevier Science Publishers, B. V.: Amsterdam, 1985; pp 125-34.
(47) Fareed, A. S.; Fang, P.; Koczak, M. J.; Ko, F. M. *Am. Ceram. Soc. Bull.* **1987**, *66*, 353-8.
(48) Mah, T.; Heicht, N. L.; Cullum, D. E. Mc.; Hoenigman, J. R.; Kim, H. M.; Katz, A. P.; Lipsitt, H. A. *J. Mater. Sci.* **1989**, *19*, 1191-201.
(49) Catoire, B.; Sotton, M.; Simon, G. Bunsell, A. R. **1984**, *Polymer* **1987**, *28*, 751-54.
(50) Sawyer, L. C.; Arons, R.; Haimbach, F.; Jaffe, M.; Rappaport, K. D. *Ceram. Eng. Sci. Proc. 7-8*, A85, 567-75.
(51) Clark, T. J.; Arons, R. M.; Stamatoff, J. B. *Ceram. Eng. Sci. Proc. 7-8*, A85, 576-88.
(52) Clark, T. J.; Jaffe, M.; Rabe, J.; Langley, N. R. *Ceram. Eng. Sci. Proc. 7-8*, A86, 901-14.
(53) Lipowitz, J.; Freeman, H. A.; Chen, R. T.; Prack, E. R. *Adv. Ceram. Mater.* **1987**, *2*, 121-28.
(54) Seyferth, D.; Wiseman, G. H.; Prud'Homme C. *Com. Am. Ceram. Soc.* **1983**, C13-C14.
(55) Legrow, J. E.; Lim, T. F.; Lipowitz, J.; Reach, R. S. *Am. Ceram. Soc. Bull.* **1987**, *66*, 363-67.
(56) Ledbetters, J. E.; Daniells, J. G.; Clemons, J. M.; Hundley, N. H.; Lenn, B. G. *J. Mater. Sci. Lett.* **1984**, *3*, 802-04.
(57) Sawyer, L. C.; Jamieson, M.; Brikowski, D.; Aider, M. I.; Chen, R. T. *J. Am. Ceram. Soc.* **1987**, *70*, 798-810.
(58) Okamura, K.; Sato, M.; Hasegawa, Y. U.S. Patent 4,650,773, Mar 1987.

fibers can be obtained from green PCS fibers when the pyrolysis treatment is performed under an atmosphere of ammonia.[59] In all these attempts, the aim often was to form an amorphous (or poorly crystallized) phase, resulting in a high tensile strength, more stable at high temperature than the commercially available fibers.

The objectives of the present work were (i) to better understand the mechanisms involved in the pyrolysis of organosilicon precursors, (ii) to characterize the pyrolytic residue, and (iii) to derive relationships between the nature of the precursor and the nature and properties of the ceramic. Our approach was to use *functional poly(carbosilane) models* better defined from a structural standpoint than those obtained according to the Yajima route.[60-62] These new PCS model precursors have been selected in order (i) to verify the *concept of branching* previously expressed by Schilling et al.[19] (according to which high ceramic yields are related to a high degree of branching of the polymeric chains), by considering model precursors with functional groups able to cross-link, (ii) to introduce *nitrogen atoms* into the precursors that may act as inhibitors in the mechanisms responsible for the coarsening of the microstructure of the pyrolytic residue at high temperature, and (iii) to increase the amount of *free carbon* in the ceramic by considering a family of precursors with different C/Si atomic ratios.

Experimental Section

The functional PCS or PCSZ models that have been selected for the present study are listed in Table I. Their synthesis and characterization have been described in detail elsewhere.[62] On the basis of the concept of branching, poly[(dimethylsilylene)methylene] (I) is of little interest as a ceramic precursor, because of its linear structure. As a matter of fact, during heating at elevated temperatures, the linear chains are broken into low molecular weight fragments leading to a very low ceramic yield at 1000 °C. In comparison, poly[(dimethylsilylene)methylene] (I) can be easily chlorinated according to eq 1 given in Figure 1. Taking advantage of the high chemical reactivity of the Si–Cl bonds in the chlorinated polymeric molecules II, new functional PCS or PCSZ species of potential interest as new precursors were prepared.

In the first series of experiments, the chlorinated polymeric chains II were cross-linked through reactions common to the Si–Cl bond. On this basis, eight models of precursors referred to as Si–Si (Na,s), Si–Si (Na,i), Si–Si (K,s), Si–Si (K,i), SiNHSi, SiNHMe, $SiNME_2$, and SiOSi were prepared (Table I).

In the second series of experiments, the Si–Cl bonds of the chlorinated polymeric molecules II were first reduced by $LiAlH_4$ to give a linear poly(silapropylene) model (III) according to eq (2) shown in Figure 1. On the basis of the hydrosilylation cross-linking reaction, two new models of precursors referred to as SiC_4Si and SiC_2ArC_2Si were prepared from butadiene and *p*-divinylbenzene, respectively (Table I).

Material Characterization. Thermogravimetric analysis (TGA): For each precursor, TGA was performed on a Perkin-Elmer TG 52 apparatus under flowing purified argon with a heating rate of 5 °C min^{-1} up to 1000 °C to study the transition between the organometallic and the resulting inorganic product.

Flash pyrolysis gas analysis (FPGA): The analysis of the gaseous species evolved during the pyrolysis of some of the precursors was performed with an analytical apparatus made of a pyrolysis microfurnace, a gas chromatograph, and a mass spectrometer.[63] The sample (0.5 mg) was rapidly heated (up to 1000 °C/min) under flowing helium up to pyrolysis temperature (i.e., T_p = 500, 700, and 1000 °C) with a platinum resistance microfurnace and then maintained at that temperature for 10 s. The gaseous species formed during the flash pyrolysis were first separated by gas chromatography (Poropack Q gas chromatography column) and then identified by mass spectrometry. The effect of heating conditions specific to flash pyrolysis on (i) the chemical composition of gases and (ii) the temperatures at which they are formed has been studied previously by Bouillon et al. for a PCS-type precursor and reported elsewhere.[64] It was established that the evolution of gases takes place in flash pyrolysis at a higher temperature, i.e., by 150 °C, with respect to what is observed for more conventional pyrolysis performed at much slower heating rates.

Bulk pyrolysis experiments: Since analyses performed on the solid residues resulting from PCS or PCSZ precursors require rather large samples, bulk pyrolysis experiments were run on 1–5-g precursor samples heated in alumina crucibles under a pressure of 1–100 kPa of argon purified over P_2O_5 and magnesium (heated at 600 °C). The samples were heated, at a ramping rate of 100 °C h^{-1} up to 700 °C and 300 °C h^{-1} beyond this limit (when necessary, a few experiments were performed up to 2300 °C), with a radiofrequency induction furnace and according to a procedure described elsewhere.[64] Unless specified, the temperature plateau was usually 30–60 min.

Elemental chemical analysis: Inorganic residues resulting from the pyrolysis of PCS or PCSZ precursors were analyzed for silicon, carbon, nitrogen, oxygen, and hydrogen at CNRS, Service Central d'Analyse, BP 22 F-69390 Vernaison. The silicon content was established by ICP (induction coupling plasma) from an aqueous solution of sodium silicate resulting from the chemical attack of the sample, with an oxidizing melt based on sodium oxide. To determine the carbon content, samples were burned at high temperature under oxygen, the resulting carbon dioxide being quantitatively analyzed by IR spectroscopy. Similarly, the oxygen ratio was established from IR spectroscopy analysis of the carbon monoxide formed during the pyrolysis of the sample at about 3000 °C, whereas that of nitrogen was derived according to a catharometric method. Finally, hydrogen was quantitatively analyzed as H_2O by IR spectroscopy after combustion of the sample at about 1000 °C under oxygen.

Infrared spectroscopy (IRS): Some of the pyrolysis residues (i.e., those corresponding to SiNHMe and $SiNMe_2$) were analyzed by IR spectroscopy, according to the conventional KBr pellet technique, on a Perkin-Elmer 983 apparatus.

Raman spectroscopy microanalysis (RSMA): Raman spectroscopy analyses were performed on fragments of pyrolysis residues, with a MOLE-type microanalyzer (Jobin-Yvon Raman spectroscopy microanalyzer). The laser beam had a wavelength of 514.5 nm. The spot size was of the order of 1 μm, the depth of sample analyzed being in range of 100 nm. For each material, at least three fragments were analyzed.

ESCA experiments: ESCA was performed with a X-ray microbeam apparatus (Al Kα wavelength; spot size 150–300 μm) under ultrahigh vacuum (133×10^{-9} Pa; (5950 Hewlett-Packard photoelectron spectrometer). The charge effect was compensated for by the use of a low-energy electron gun. Each sample was Ar^+ ion etched to ensure a clean surface, prior to analysis. A semiquantitative analysis, based on the measurements of the area of the Si 2p, C 1s, and N 1s peaks (high-resolution mode) was performed for some of the pyrolysis residues. Conventional correction factors were applied. The best conditions for semiquantitative analysis of the chemical bonds were found to be a 150-μm spot size, an energy window of 25 eV, and a counting time of 8 h. As a matter of fact, it was observed that the peak width at midheight was not significantly modified by the latter parameter, for both the Si–C and C–C bonds.

X-ray diffraction (XRD): The XRD spectra (Cu Kα) were recorded from the pyrolysis residues (reduced to a fine powder by grinding) with an X-ray diffractometer (Philips PW 1710 diffractometer control). The mean apparent grain size was calculated, from the peak width measured at midheight, according

(59) Okamura, K.; Sato, M.; Hasegawa, Y.; Amano, T. *Chem. Lett.* **1984**, 2059–60.
(60) Bacque, E.; Pillot, J.-P.; Birot, M.; Dunogues, J. *Macromolecules* **1988**, *21*, 30–34.
(61) Bacque, E.; Pillot, J.-P.; Birot, M.; Dunogues, J. *Macromolecules* **1988**, *21*, 34–38.
(62) Bacque, E.; Pillot, J.-P.; Birot, M.; Dunogues, J.; Bouillon, E.; Pailler, R.; Naslain, R. *Chem. Mater.*, previous article in this issue.
(63) Sarthou, J.-C. University Thesis No. 155, Bordeaux, 1984.
(64) Bouillon, E.; Langlais, F.; Pailler, R.; Naslain, R.; Sarthou, J. C.; Delpuech, A.; Laffon, C.; Lagarde, P.; Cruege, F.; Huong, P. V.; Monthioux, M.; Oberlin, A. *J. Mater. Sci.*, Submitted.

Table II. Yield in Solid Residue at 1000 °C of the PCS and PCSZ Model Precursors.

model precursor	yield in solid residue, wt %	model precursor	yield in solid residue, wt %
Si–H	5	SiNHSi	37
SiH[a]	85	SiNHMe	24
Si–Si (Na, s)	11	$SiNMe_2$	33
Si–Si (Na, i)	77	SiOSi	54
Si–Si (K, s)	43	SiC_4Si	14
Si–Si (K, i)	59	SiC_2ArC_2Si	24

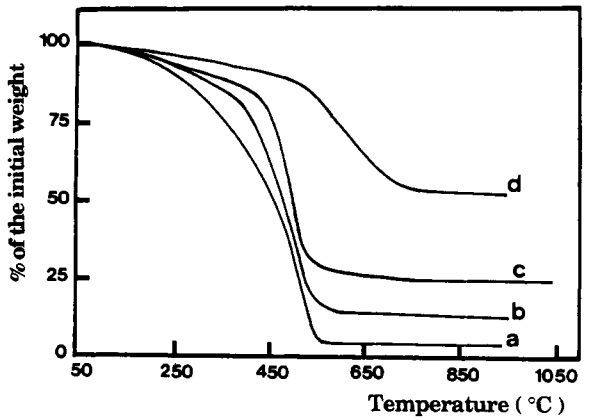

Figure 2. TGA of the weight loss observed during the pyrolysis of PCS precursors: (a) Si–H; (b) SiC_4Si; (c) SiC_2PhC_2Si; (d) SiOSi.

to the Scherrer equation. It was assumed that the only cause of peak broadening was that related to the grain size, i.e., those due to microstraining and sample inhomogeneity were neglected.

Results and Discussion

The Organometallic–Inorganic Transition. As identified from the TGA analyses: The *Si-H precursor model*, referred to as model III in Figure 1, i.e., poly(silapropylene), exhibits a progressive thermal decomposition that is almost complete by 560 °C with a very low ceramic yield (Figure 2a and Table II). This result is expected due to the lack of branching in this precursor model.[62] Due to its pure linear structure, the polymeric chain fragments, during pyrolysis, form very low molecular weight species. In contrast, when this precursor model was treated *in an autoclave at 450 °C*, it became progressively insoluble and its pyrolysis gave rise to high ceramic yields, as shown in Table II. It is thought that a considerable amount of rearrangement and branching occurs during the autoclave thermolysis step (as a matter of fact some of the Japanese PCSs used for the preparation of NICALON-type fibers were treated in this way to obtain an acceptable ceramic yield). Thus, these data confirmed the relation between the degree of branching of the polymeric precursor and the pyrolysis yield, as previously reported by Schilling et al.[19]

The autoclave thermolysis destroyed the well-characterized structure of the starting model precursor, but it resulted in a significant increase in the residue yield of the pyrolysis.

The thermal behavior of the various *Si–Si precursors* is shown in Figure 3. As far as the soluble fractions(s) of the precursors are concerned, the Si–Si (K, s) precursor exhibited a progressive organometallic–inorganic transformation that starts at about 400 °C and ends at about 700 °C. On the contrary, the Si–Si (Na, s) precursor shows a sharp transition at about 400 °C. Furthermore, the ceramic yields (Table II) are rather different but remain low, i.e., 11% for Si–Si (Na, s) and 43% for Si–Si (K, s). The ceramic yields for the insoluble fractions are much higher, i.e., 59% for Si–Si (K, i) and 77% for Si–Si (Na, i). This result is in good agreement with the fact that the degree of cross-linking is higher for the insoluble fractions than for their soluble counterparts. Thus, a rather high degree of cross-linking results again in a high yield in solid residue even when pyrolysis was achieved in the presence of thermally weak disilane bonds.

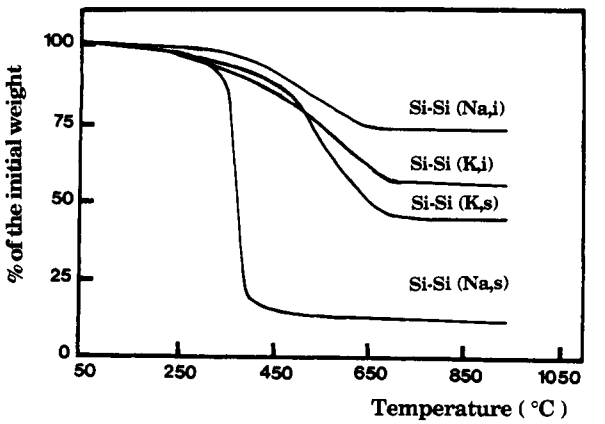

Figure 3. TGA of the weight loss observed during the pyrolysis of various PCS Si–Si precursors.

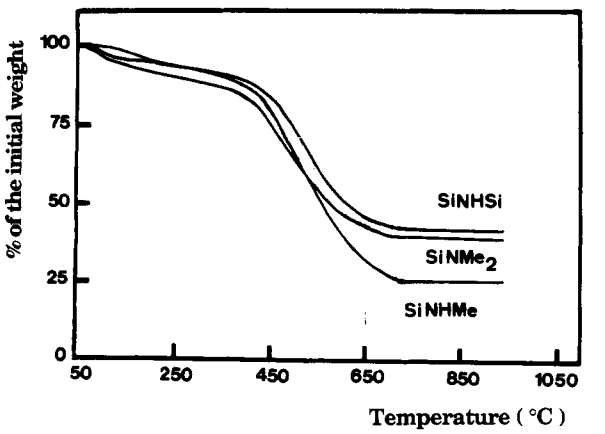

Figure 4. TGA of the weight loss observed during the pyrolysis of various PCSZ precursors.

The SiC_4Si and SiC_2ArC_2Si model precursors were characterized by organometallic–inorganic transformations that were essentially complete at about 550 °C and result in low ceramic yields (14% and 24% for SiC_4Si and SiC_2ArC_2Si, respectively). On the contrary, the SiOSi model precursor was characterized by a rather high ceramic yield (54%). As expected, the hydrocarbon chemical bridges appeared to be much weaker than the oxygen ones (Figure 2).

As shown in Figure 4, the PCSZ ceramic yields depend on the structure of the model precursors. When the precursor is only weakly cross-linked, i.e., when its structure is built mainly from cycles resulting from intramolecular cyclizations, the yield of solid residue is very low. On the other hand, when the precursor was characterized by more cross-linking, the yield of solid residue was higher. As an example, a PCSZ that had been obtained without solvent by reaction between poly[(chlorosilylene)methylene] and methylamine (to promote intermolecular cyclization mechanisms and thus cross-linking) gave a high residue yield, i.e., 53%, a result that has to be compared with that (i.e., 24%) given in Table II for the PCSZ precursor model SiNHMe obtained in CH_2Cl_2 as the solvent.

Generally speaking, it appears that the PCS and PCSZ precursor models here considered do not result in high yields in solid residue (with the exception of SiOSi).

Table III. Gaseous Species Resulting from the Pyrolysis at Different Temperatures of Various PCS and PCSZ Precursors (Flash Pyrolysis)[a]

nature of precursors	temp, °C		
	500	700	1000
SiNHSi	butene	methane butene	methane butene
SiNHMe	methane ethene methoxytrimethylsilane	methane ethene tetramethylsilane methoxytrimethylsilane	methane ethene
$SiNMe_2$	trimethylsilane trimethylamine	methane trimethylamine	methane ethene
Si–H	methane	methane dimethylsilane trimethylsilane tetramethylsilane	methane ethene dimethylsilane tetramethylsilane

[a] It should be mentioned that hydrogen, not analyzed by mass spectroscopy, it also present (as well as heavy polymeric species due to an early condensation).

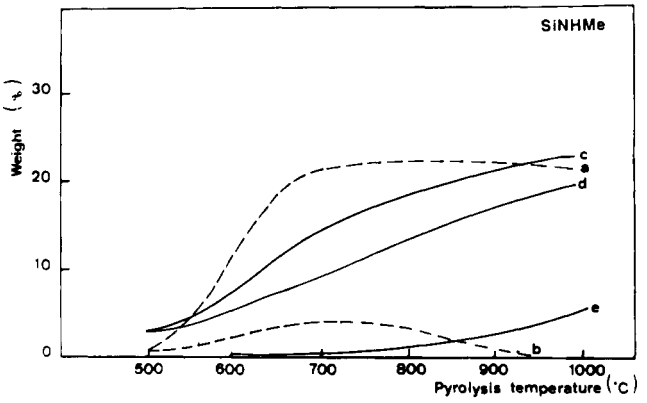

Figure 5. Variation of the mass of the gaseous phase evolved from 100 g of precursor for the species tetramethylsilane (a), trimethylsilane (b), ethene (c), methane (d), and butene (e).

However, this conclusion is no longer true when the structure of the polymer moves by cross-linking to a three-dimensional network through strong Si–O–Si or Si–N–Si bonds (and not weak hydrocarbon bridges).

Results of gas analyses: The gases formed during the flash pyrolysis of Si–H, SiNHSi, SiNHMe, and $SiNMe_2$ were analysed by gas chromatography/mass spectrometry for three temperatures of the platinum resistance microfurnace, 500, 700, and 1000 °C. The main gaseous species that have been unambiguously identified are alkanes (methane, ethane, etc.) alkenes (ethene, butene, etc.), and various methylsilanes. In addition, during the pyrolysis of PCSZ precursors, different gaseous species containing nitrogen also were formed, such as acetonitrile, propionitrile, and trimethylamine. Finally, one must mention the occurrence of products with higher molecular weights (which are thus difficult to detect due to their early condensation on the cold wall) as well as hydrogen (Table III).

Evolution of the relative amount of each main gaseous species, as a function of the pyrolysis temperature, has been tentatively plotted in Figures 5–7. It clearly appears that at 350 °C (or 500 °C without correction), the thermal decomposition is still very limited for most PCS or PCSZ precursors. These results are in good agreement with that of TGA experiments taking into account the temperature shift of about 150 °C between flash pyrolysis and TGA pyrolysis (i.e., flash pyrolysis experiments performed at 500 °C must be compared with TGA experiments run at

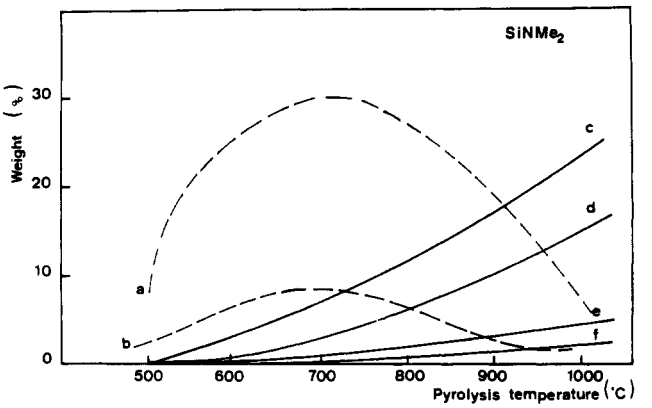

Figure 6. Variation of the mass of the gaseous phase evolved from 100 g of precursor for the species tetramethylsilane (a), trimethylamine (b), methane (c), ethene (d), ethane (e), and butene (f).

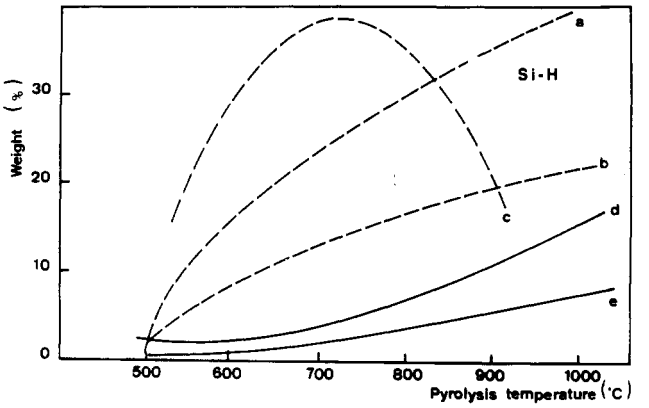

Figure 7. Variation of the mass of the gaseous phase evolved from 100 g of precursor for the species trimethylsilane (a), dimethylsilane (b), tetramethylsilane (c), methane (d), and ethylene (e).

Table IV. Weight Loss at Different Stages of the Thermal Treatment of PCS and PCSZ Precursors

	$\Delta m/m$, %		
	T = 350 °	T = 550 °C	T = 850 °C
SiH	23	88	95
SiNHSi	8	33	62
SiNHMe	9	54	75
$SiNMe_2$	9	53	66

350 °C to take into account the kinetics of the decomposition) (Table IV).

On the contrary, at 550 °C (or 700 °C without correction), the relative amounts of gas were significant regardless of the nature of the precursor. Obviously, this temperature fell within the temperature range where the organometallic–inorganic transformation occurs. This result was again in good agreement with that of the TGA analysis performed at 550 °C. Therefore, under such temperature conditions, the thermal degradation of most of the precursors was already very significant (in fact it was almost fully achieved for the Si–H precursor). At these temperatures, the polymeric chains are broken, their fragments giving silicon- or carbon-based gaseous or low molecular weight species after intramolecular rearrangements. It is thought that these phenomena may involve free radicals whose presence would allow numerous recombinations leading to gas formation. As an example, the formation of trimethylamine during the pyrolysis of $SiNMe_2$ could result from the recombination of $^{\bullet}NMe_2$ with $^{\bullet}Me$. So, incorporating nitrogen in the lateral groups as in $SiNMe_2$

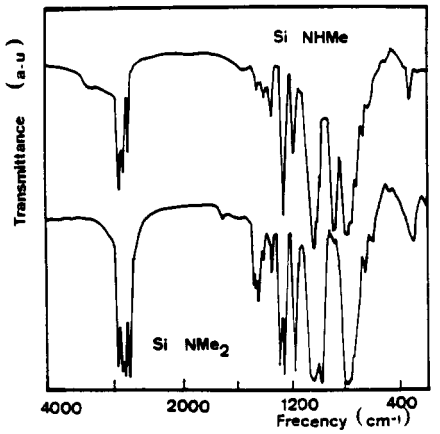

Figure 8. IR spectra of the SiNHMe and $SiNMe_2$ precursors.

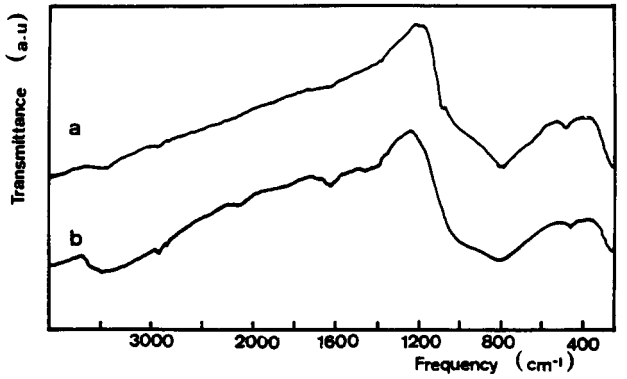

Figure 9. IR spectra of the SiNHMe and $SiNMe_2$ precursor pyrolysed at (a) 1000 and (b) 700 °C.

(see Table I) does not seem favorable for elaborating a nitrogen-based ceramic.

Finally at 850 °C (or 1000 °C without correction), flash pyrolysis gave rise to gaseous species that could result from recombinations between free radicals though to be less numerous than at 550 °C (or 700 °C without correction). The gas evolution at this temperature, which may be considered as the end of the organometallic–inorganic transformation, was still significant (particularly for the Si–H precursor, as shown in Figure 7).

As identified from the IR analysis: The occurrence of an organometallic–inorganic transformation during the pyrolysis of PCS and PCSZ precursors, which had been already identified from TGA and gas analysis, was further studied by IR spectroscopy for the SiNHMe and $SiNMe_2$ precursors.

As shown in Figures 8 and 9, the absorption bands corresponding to the organic bonds characteristic of the starting SiNHMe and $SiNMe_2$ precursors almost completely disappeared at a pyrolysis temperature of 700 °C. For higher pyrolysis temperatures, i.e., for $700 < T_p < 1000$ °C, the IR spectrum of the solid residue undergoes slight changes, its main features being maintained. As an example, for the $SiNMe_2$ precursor, the IR spectrum exhibits, for $T_p = 700$ °C, a broad absorption band at 820 cm^{-1} that has been assigned to SiC_4 tetrahedral species (Figure 9). For $T_p = 1000$ °C, the SiC absorption band is narrower and better defined, whereas a shoulder is observed on its left side at 1100 cm^{-1}, which could be assigned to Si–O bonds. IR spectrum of silicon nitride exhibits a strong Si–N absorption band at 950 cm^{-1}, which could be mixed with those due to Si–C and Si–O bonds in the pyrolysis residue of PCSZ precursors, and a weaker absorption band at 490 cm^{-1}, which is more convenient to identify Si–N bonds. As shown in Figure 9, such a weak absorption band is present in the pyrolysis residue of $SiNMe_2$ for both $T_p = 700$ and 1000 °C. Assuming that it could be assigned to Si–N bonds, it appears that the three expected Si–C, Si–O, and Si–N bonds are present in the solid residue formed during the pyrolysis at 700–1000 °C of PCSZ precursors.

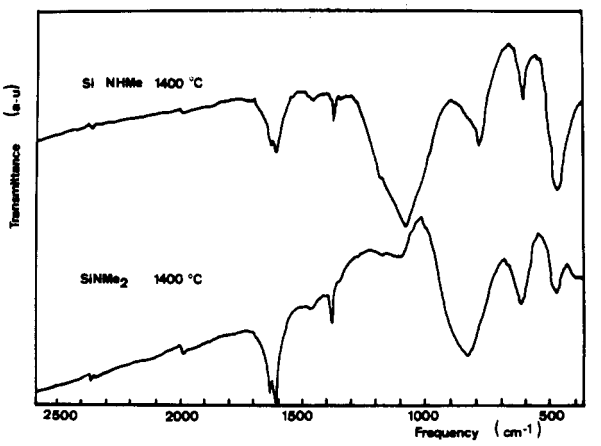

Figure 10. IR spectra of SiNHMe and $SiNMe_2$ precursors pyrolyzed at 1400 °C.

Table V. Chemical Composition (at. %) of the Solid Residues of PCS and PCSZ Precursors Pyrolyzed at 1200 °C

precursors	Si	C	N	O	H
$SiNMe_2$	30.0	42.6	10.5	13.9	2.8
SiNHMe	30.8	42.2	11.5	14.5	1.8
SiNHSi	30.7	39.9	12.3	14.2	2.3
SiSi (Na, s)	32.3	42.8		24.4	1.0
SiOSi	31.7	42.2		23.0	2.1
SiH[a]	32.5	43.3		21.2	2.9

[a] Heated at 450 °C in autoclave and then pyrolyzed at 1200 °C.

At higher pyrolysis temperatures, i.e., $T_p = 1400$ °C, the occurrence of SiC becomes more apparent again. In the solid residue formed during the pyrolysis of $SiNMe_2$, the strong absorption band at 830 cm^{-1} can be assigned to tetrahedral Si–C bonds. As discussed above, the weak absorption bands at 490 and 1100 cm^{-1} could be assigned to Si–N and Si–O bonds (Figure 10). Furthermore, on the basis of the results of a study by Guiliano et al., the absorption bands at 1600 and 1380 cm^{-1} could be assigned respectively to C=C bonds in aromatic and to CH_3.[65]

Elemental Analysis of the Pyrolytic Residues. Overall elemental analyses: Chemical compositions of the solid residues formed during the pyrolysis of the PCS and PCSZ precursors at 1200 °C are given in Table V and prompt the following remarks:

(i) It is noteworthy that *hydrogen* was still present in the material even for $T_p = 1200$ °C, i.e., at a temperature well above the end of the organometallic–inorganic transformation (this amount of hydrogen could contribute to the stabilization of "amorphous" SiC states as already known for amorphous silicon).

(ii) All the solid residues contained *significant amount of oxygen* (very likely bonded to silicon). Since the initial PCS and PCSZ contained about 3 wt % oxygen, this feature suggests that contamination by oxygen occurred during pyrolyses themselves due to (1) the high affinity of PCS and PCSZ for oxygen and moisture and (2) the small volume of the samples submitted to pyrolysis with

(65) Guiliano, M.; Mille, G.; Kister, J.; Dou, H. J. M. *Analusis* **1984**, *12*, 201–4.

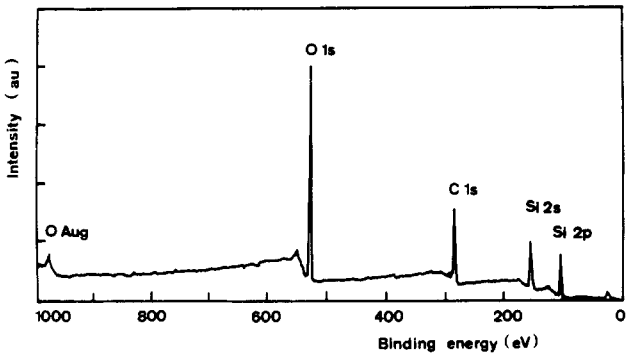

Figure 11. ESCA spectrum of ex-Si–Si (Na, s) pyrolytic residue (T = 1200 °C).

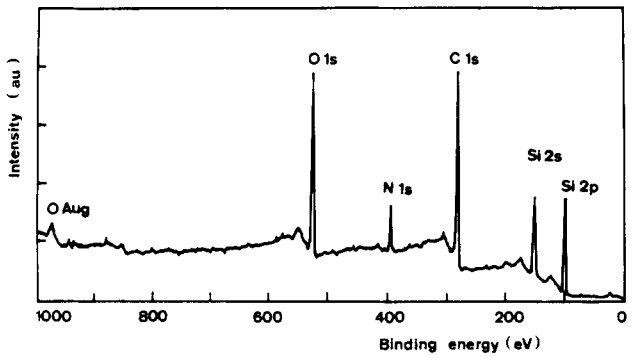

Figure 12. ESCA spectrum of ex-SiNHMe pyrolytic residue (T = 1200 °C).

respect to the volume of gas adsorbed on the inner parts of the pyrolysis apparatus.[64] Less contamination by oxygen would have been observed with larger samples.

(iii) Finally, assuming that oxygen and nitrogen are bonded to silicon as binary SiO_2 and Si_3N_4 species, i.e., neglecting the occurrence of ternary or quaternary silicon-based species, the data given in Table V suggest that the pyrolytic residues formed at 1200 °C may contain a significant amount of free carbon.

ESCA analyses: Generally speaking, the ESCA spectra of inorganic residues formed by pyrolysis of PCS and PCSZ precursors exhibit sharp peaks that have been assigned to silicon (Si 2s and 2p), carbon (C 1s), oxygen (O 1s), and nitrogen (N 1s), as illustrated in Figures 11 and 12. Furthermore, when in the high-resolution mode, these peaks can be used after decomposition to assess the nature and relative amounts of the chemical bonds. As a matter of fact, each peak (i.e., Si 2p, C 1s, and N 1s) recorded for these ex-PCS or ex-PCSZ solids could be analyzed on the basis of the same components but with different intensities (Figure 13 and 14):

(i) Si 2p peaks could be assigned to three components. The first, at 98 eV (or 100.8 eV when a charge effect correction is applied), was assigned to the Si–C bond in silicon carbide. The second, at 100.8 eV (or 103.5 eV after correction), is related to the Si–O bond in silica. Finally, the third, which fell at an intermediate position in the binding energy axis, could be assigned to silicon atoms bonded either simultaneously to both carbon and oxygen atoms (ex-PCS) or as well as to nitrogen atoms (ex-PCSZ).

(ii) C 1s peaks could be explained by the presence of at least two components. The first, 279.7 eV, and the second, at 281.1 eV (or 282.7 and 284.1 eV after correction), were assigned to the C–Si bonds in Si–C and C–C bonds (and to a small extent to C–H bonds) in free carbon, respectively. The others components at higher positions on the binding energy axis could be related to C–O bonds from

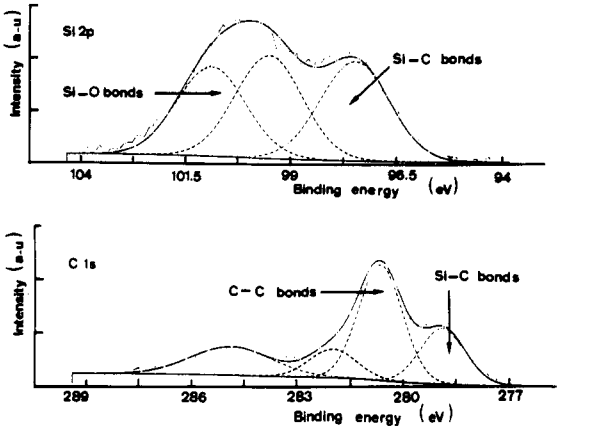

Figure 13. Deconvolution of the ESCA Si 2p and C 1s peaks of ex-Si–Si (Na, s) pyrolytic residue (T = 1200 °C).

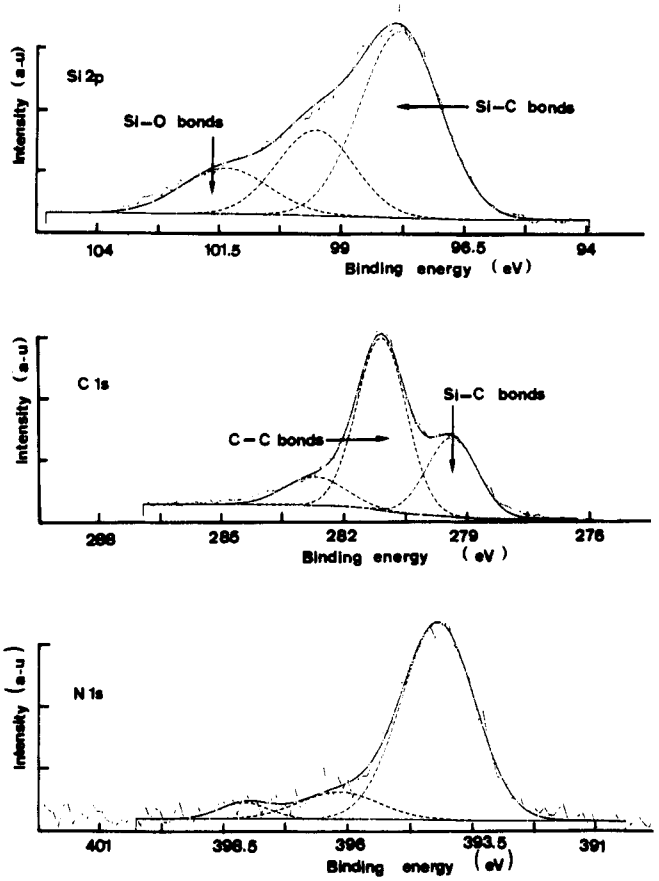

Figure 14. Deconvolution of the ESCA C 1s, Si 2p, and N 1s of ex-SiNHMe pyrolytic residue (T = 1200 °C).

CO and CO_2 molecules adsorbed on the sample surface (due to an insufficient cleaning treatment of the surface prior to the analysis).

(iii) Analysis of the N 1s peaks (for the ex-PCSZ) shows a component at 394.5 eV (see Figure 14) corresponding to a binding energy similar to that characterizing Si–N bonds in Si_3N_4. This result suggests that nitrogen is bonded to silicon in the ex-PCSZ as it is in silicon nitride.

(iv) Finally, the analysis of the O 1s peaks could not be performed due to too small chemical shifts among the binding energies related to the different oxygen-containing species.

Despite the complexity of the Si 2p, C 1s, and N 1s peaks due to that of the materials themselves, elemental composition of the ex-PCS and ex-PCSZ residues (for T_p = 1200 °C) were assessed semiquantatively. Results of the

Table VI. Elemental Atomic Percentages (Overall and per Chemical Bond) in the Inorganic Solids Resulting from the Pyrolysis at 1200 °C of PCS and PCSZ Precursors, As Semiquantitatively Derived from the Component Intensities of ESCA Peaks

	Si, at. %			C, at. %			N, at. %		
nature of precursor	SiC	SiX	SiO	C–Si	C–C C–H	C–O C=O	Si–N	1	
$SiNMe_2$		23.9			44.5		7.2		25.3
	14.6	6.7	2.6	10.3	29.4	4.8	6.4	0.8	
SiNHMe		25.6			36.6		5.5		32.2
	13.8	6.7	5.1	10.8	31.8	4.0	4.5	1.0	
SiNHSi		25.1			37.8		6.1		30.7
	14.6	6.1	4.4	10.6	22.6	4.6	5.0	1.1	
Si-Si (Na, s)		21.4			31.9				46.8
	7.4	7.4	6.6	7.3	13.9	10.7			
SiOSi		23.7			30.6				45.6
	10.7		13.0	8.4	16.7	5.53			45.6

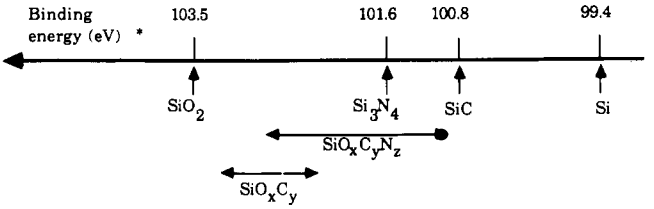

(*) Charge effect correction is applied

Figure 15. Binding energies (Si 2p) in binary and ternary tetratredral species containing silicon (schematic), as derived from ESCA analysis.

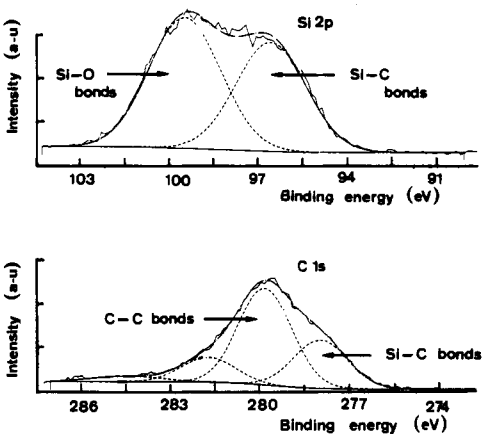

Figure 16. Deconvolution of the ESCA Si 2p and C 1s peaks of ex-SiOSi pyrolytic residue (T = 1200 °C).

calculations are given in Table VI as (i) the atomic percentages of silicon, carbon, nitrogen, and oxygen present in the various materials and (ii) for each element, the atomic percentage involved in each chemical bond discussed above. The calculations have taken into account the occurrence of complex intermediate species. Such complex species had been already mentioned by Bouillon et al.,[64] Sawyer et al.,[66] and Lipowitz et al.[53] and are referred to as SiO_xC_y or Si-X, for the rather simple case of the ex-PCS solids. A silicon oxycarbide has been very recently identified by ESCA analyses in Nicalon fibers themselves.[39,67] The situation was still more complicated for the ex-PCSZ solids due to nitrogen. On the one hand, it seems well established that a significant amount of nitrogen is bonded to silicon as it is in Si_3N_4 (i.e., SiN_4 tetrahedron, Figure 14). On the other hand, a small amount of nitrogen also may be involved in complex SiO_xN_y or $SiO_xC_yN_z$ tetrahedral species. The chemical shifts related to these tetrahedral complexes remain unknown but probably fall within a binding energy range limited by SiO_2 and SiC, as schematically shown in Figure 15. As a result, the intermediate component observed by decomposition of the Si 2p peak could be a mixture of different complex tetrahedral species, a feature that makes a quantitative analysis very difficult.

The contamination by oxygen of the ex-PCS and ex-PCSZ solids already established from the results of the overall chemical analysis, is also apparent from Table VI. The higher oxygen percentages obtained from ESCA peaks could be explained by the occurrence of oxygen-containing molecules adsorbed on the sample surface, as discussed above.

Surprisingly, the deconvolution of the Si 2p peak observed for the ex-SiOSi solid did not lead to an intermediate component (related to ternary tetrahedral SiC_xO_y species) between those assigned to the Si–C and Si–O bonds, as shown in Figure 16. This result suggests that the Si–O bonds initially present in the SiOSi precursor could directly give rise to tetrahedral SiO_4 species in the pyrolytic residue. Therefore, the ternary tetrahedral SiC_xO_y species observed in some of the other pyrolytic residues may have their origin in C–Si–O bonds formed during the synthesis and/or at the beginning of the pyrolysis of those precursors.

Table VII. Massic Concentrations (wt %) of the Various Species Present in Inorganic Residues Obtained by Pyrolysis at 1200 °C of Some PCS and PCSZ Precursors, As Calculated from the Results of ESCA Analysis (Neglecting the Occurrence of Complex Tetrahedral Ternary or Quaternary Species)

nature of precursor	SiC	SiO_2	C	Si_3N_4
SiSi (Na, s)	34	23	20	
SiNHSi	38	23	24	14
SiNHMe	38	26	23	13
$SiNMe_2$	38	13	31	17

Finally, the chemical composition of the ex-PCS and ex-PCSZ pyrolytic residues, expressed as SiC, "SiO_2", free carbon, and Si_3N_4 weight percentages, was derived from the ESCA data, neglecting the occurrence of the ternary or quaternary tetrahedral species. The amounts of SiC, SiO_2, and free carbon were calculated from the Si 2p and C 1s peak components and that of Si_3N_4 from the N 1s peak, as discussed above. Results are given in Table VII. It clearly appears that the SiC percentage in the inorganic residue is almost the same whatever the nature of the precursor was. Furthermore, the SiO_2 and free carbon percentages calculated for the ex-$SiNMe_2$ pyrolytic residue are respectively lower and higher than those obtained for the other materials. This result could be explained by the fact that the $SiNMe_2$ precursor has a lower cross-linking capability and then less sites to fix oxygen atoms during the first part of the pyrolysis, i.e., between 200 and 500 °C.

(66) Sawyer, L. C.; Chen, R. T.; Haimback, F.; Hargert, P. J.; Pracks, E. R.; Jaffe, M. *Ceram. Eng. Sci. Proc.* **1986**, *7*, 914.
(67) Porte, L.; Sartre, A. *J. Mater. Sci.* **1989**, *24*, 271–275.

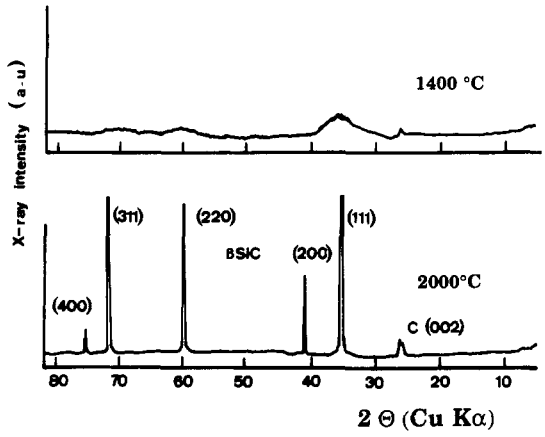

Figure 17. X-ray diffraction patterns of the solid resulting from the pyrolysis of SiNHSi under argon flow.

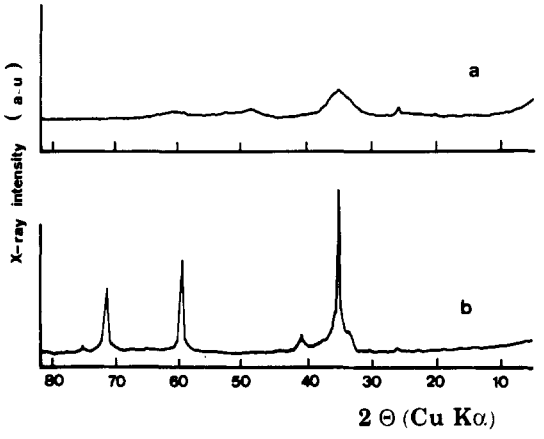

Figure 18. X-ray diffraction patterns of the solid resulting from the pyrolysis of $SiNMe_2$: (a) under argon flow at 1400 °C; (b) under vacuum (133×10^{-6} Pa at 1400 °C).

Structure and Microstructure of the Pyrolytic Residues. From XRD analyses: When heated for 1 h under argon flow (P = 100 kPa), according to a procedure described elsewhere,[64] the solid residue resulting from the organometallic–inorganic transformation remained *amorphous* up to 1400 °C for the SiNHSi, SiNHMe, and $SiNME_2$ precursors, as shown in Figures 17 and 18a. In contrast, when treated under the same conditions, the pyrolytic residue of the Si–Si (Na, s) precursor was characterized by broad XRD lines: three assigned to cubic β-SiC ((111), (220), and (311)) and one (002) to pyrocarbon, as shown in Figure 19. As a matter of fact, the state of crystallization in this latter case was comparable to that of the SiC–based fiber (obtained from a related PCS precursor), the apparent mean grain size (calculated according to the Scherrer's equation) being of the order of 3 nm. When heated at higher temperatures, e.g., 1600 °C, the ex-Si–Si (Na, s) ceramic was better crystallized, as shown by narrower XRD peaks and a larger mean grain size (15 nm).

Furthermore, thermal treatment at 1400 °C for 1 h, when performed under high vacuum (133×10^{-6} Pa) led, for all the nitrogen-based precursors, to ceramics in which the β-SiC phase was well crystallized (mean grain size larger than 100 nm), as shown in Figure 18b for $SiNMe_2$. Moreover, under these conditions, the oxygen concentration in the pyrolytic residue was only 8 at. % (instead of 14 at. % when treated under argon flow). From these results, it seems that the simultaneous presence of the oxygen and nitrogen heteroatoms inhibited the grain growth of β-SiC.

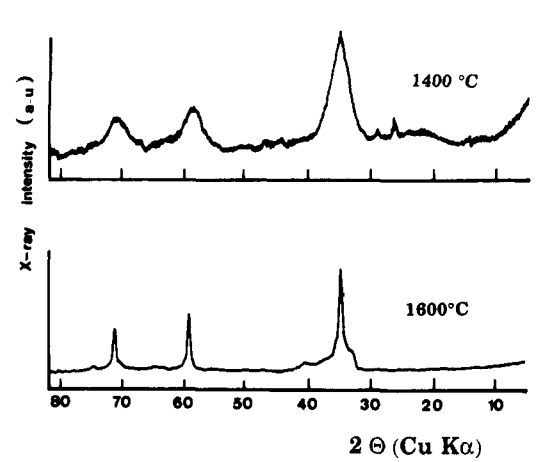

Figure 19. X-ray diffraction patterns of the solids resulting from the pyrolysis of Si–Si (Na, s) precursors, under argon flow.

As expected, a thermal treatment under argon flow at very high temperatures, i.e., 2000 °C, improved the state of crystallization of the β-SiC phase, as shown in Figure 17 for SiNHSi. However, even under such conditions the XRD lines of Si_3N_4 were not observed. On the contrary, the 002 line of carbon was clearly apparent with a d value of 3.42 Å. Assuming that $d(002)$ is respectively equal to 3.44 Å for a fully disordered carbon and 3.35 Å for graphite, the degree of disorder g of a carbon is often defined as[68]

$$g = l[(3.44 - d(002)_{obs})/(3.44 - 3.35)] \quad (1)$$

On the basis of the d value measured from the XRD pattern shown in Figure 17, bottom, the degree of disorder of carbon in the ex-SiNHSi ceramic treated at 2000 °C under argon, as calculated from eq 1 is only 20%. Furthermore, the apparent mean grain size along the c axis, as calculated from the 002 peak width at midheight according to the Scherrer's equation, was of the order of 9 nm, a value that corresponds to a stack of about 25 graphitic layers. Therefore, one may conclude that the carbon phase in ceramics derived from nitrogen-containing precursors is rather well crystallized when they have been treated at 2000 °C under argon flow.

From Raman spectroscopy microanalysis (RSMA): Raman spectroscopy is known to be a suitable method to characterize poorly crystallized solids (e.g., materials prepared at low temperatures). As an example, it has been used to study SiC CVD filaments[69,70] as well as SiC-based yarn fibers derived from PCS precursors.[71] RSMA was particularly successful in the characterization of the poorly graphitized carbon present in such materials.

In the present study, the RSMA has been used to characterize the ceramics obtained by pyrolysis of various PCS (i.e., Si–Si (Na, s)) and PCSZ (i.e., SiNHSi, SiNHMe, and $SiNMe_2$) precursors, performed at 1400 °C under argon flow (100 kPa) for 1 h. Some of the Raman spectra are shown in Figure 20. Their main features are (i) two strong peaks between 1300 and 1600 cm^{-1}, (ii) one (or two) weak peak(s) between 2500 and 3000 cm^{-1}, and (iii) a complex broad band between 500 and 1000 cm^{-1} whose shape and intensity are different from one material to another.

(68) *Les Carbones*; edited by le Groupe Français d'Etude des Carbones, Masson, 1965; Tome 1.
(69) Gorman, M.; Solin, S. A. *Solid State Commun.* **1974**, *15*, 761.
(70) Morimoto, A.; Kutaoka, T.; Kumada, M.; Schimiza, T. *Philos. Mag. B* **1984**, *50*, 5.
(71) Martineau, P.; Layaye, M.; Pailler, R.; Naslain, R.; Couzi, M.; Cruege, F. *J. Mater. Sci.* **1984**, *19*, 2731.

Table VIII. Wavenumber of the Raman Peaks for Solid Residues Resulting from the Pyrolysis of Various Precursors in Wavenumber Ranges That May Correspond To Silicon Carbide (a), Carbon First Order (b), and Carbon Second Order (c)

		wavenumber ν, cm^{-1}					
		a		b		c	
nature of precursor	T(pyr), °C						
phenolic resin	1400			1350	1590	2700	
SiSi (Na, s)	1400	750	950	1350	1600	2650	2890
$SiNMe_2$	1400	780	1000	1350	1590	2650	2890
SiNHSi	1400	780	910	1350	1605	2650	2905
SiNHMe	1400	750		1350	1600		
	1600	780		1350	1585	2670	2870
	1700	700		1350	1580	2670	
	1800	800	1080	1350	1580	2694	
	2000	800	1100	1350	1575	2694	
	2300	780	980		1580	2720	

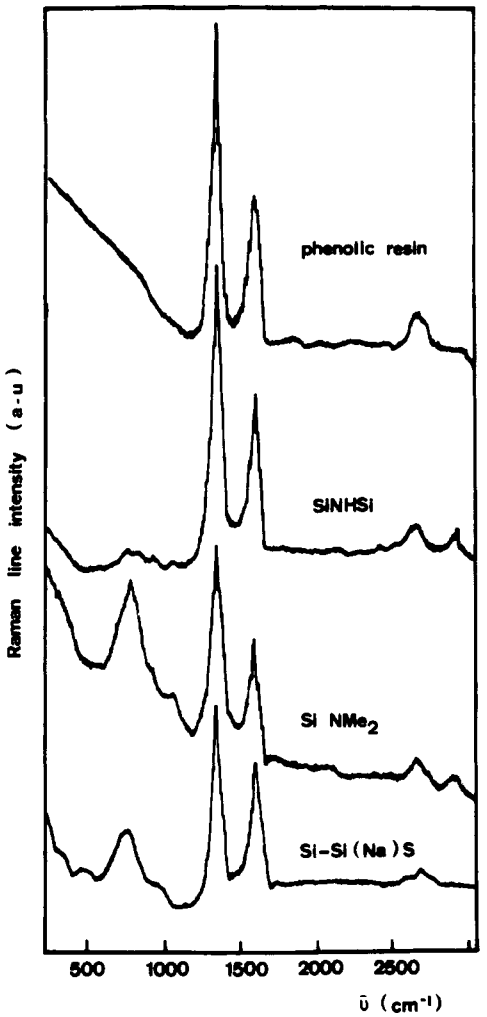

Figure 20. Raman spectrum of the residue resulting from the pyrolysis at 1400 °C of various precursors.

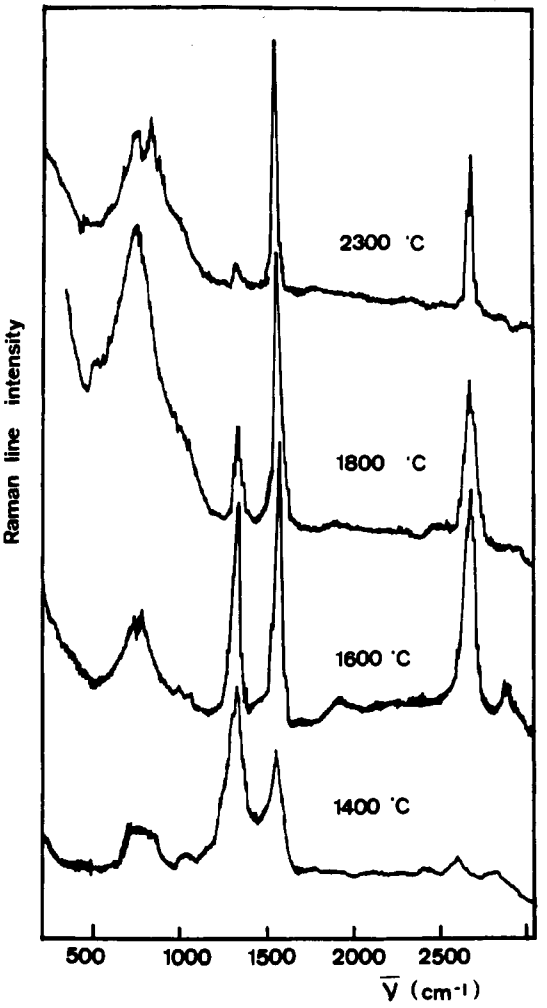

Figure 21. Evolution with T_p of the Raman spectra of the solid residue resulting from the pyrolysis of the SiNHMe precursor.

The above-mentioned peaks in i and ii were assigned to *free carbon* by reference to the literature.[72-76] In contrast, assignment of that (or those) falling in the 500–1000-cm^{-1} range remains uncertain. Since the Raman peaks due to carbon were known to be sensitive to the degree of graphitization of carbon,[75] the residue of the organometallic–inorganic transformation for SiNHMe was heat treated under argon flow at increasing temperatures up to 2300 °C. The corresponding Raman spectra, given in Figure 21, show that the heat treatment has (i) modified the intensity and width of all the peaks and (ii) resulted in slight shifts of their positions in the wavenumber scale (Table VIII). It appears from the literature that most of these features may be related to the graphitization of the poorly crystallized carbon formed during the organometallic–inorganic transformation.

A detailed analysis of the Raman spectra of pyrolytic carbons (assignment of the peaks, evolution of their wavelength numbers, and relative intensities with the state of graphitization) has been the subject of several studies and still remains a controversial matter.[72-76] The Raman

(72) Sasaki, Y.; Nishima, Y.; Sato, M.; Okamura, K. *J. Mater. Sci.* **1987**, *22*, 443–448.
(73) Tuinstra, F.; Koenig, J. L. *J. Chem. Phys.* **1970**, *33*, 1126.
(74) Rouzaud, J. N.; Oberlin, A.; Bassez, C. B. *Thin Solid Films* **1983**, *105*, 75–96.
(75) Lespade, P.; Marchand, A.; Couzi, M.; Cruege, F. *Carbon* **1984**, *22*, 375.
(76) Galiotis, C.; Batchelder, D. N. *J. Mater. Sci. Lett.* **1988**, *7*, 545–7.

spectrum of a pyrolytic carbon usually consists of two peaks of strong intensity at 1350 and 1578–1600 cm^{-1} (first order) and one broad peak of weaker intensity at 2700 cm^{-1} (second order). The peak at 1578 cm^{-1}, also observed for graphite, was identified with the doubly degenerate deformation mode of the hexagonal ring structure having E_{2g} symmetry.[76] The appearance of the forbidden peak at 1350 cm^{-1} of A_{1g} symmetry (which is not observed for graphite single crystals) was attributed to the breakdown of translational symmetry, caused by the presence of in-plane defects located between adjacent basic structural units (BSUs) of carbon responsible for the existence of tilt and twist boundaries.[74-76] As graphitization proceeds (i) the E_{2g} peak shifted from 1600 to 1578 cm^{-1}, (ii) the relative intensity of the A_{1g} peak decreased, and (iii) the peak became sharper.

As shown in Figure 20, the Raman spectra of carbon present in the pyrolytic residues of PCS and PCSZ obtained at 1400 °C were not very different from that of carbon resulting from the pyrolysis of a phenolic resin (performed under the same conditions). The strong intensity of the A_{1g} peak suggested the occurrence of numerous in-plane defects, as could be expected. Furthermore, the Raman spectra presented in Figure 21 and the data listed in Table VIII clearly show the progression of the graphitization of carbon in the ex-PCSZ residues, as the temperature of pyrolysis increases from 1400 to 2300 °C with, as mentioned above, (i) a decrease in intensity of the A_{1g} peak whose intensity becomes almost nil for T_p = 2300 °C (as the in-plane defects are eliminated) and (ii) a shift of the E_{2g} peak from 1600 to 1580 cm^{-1}.

Graphitization of carbon ex-PCS or ex-PCSZ residues could be followed, as it proceeds, by plotting the variations of the Raman peak intensity ratios, i.e., $I(1350)/I(1600)$ and $I(2700)/I(1600)$ versus T_p. However, one should mention that the accurate measurements of the intensity of a Raman peak is particularly difficult for carbon (since the orientation of the carbon microcrystals with respect to the laser beam must be taken into account due to polarization effects). Therefore, the measurements were performed, for each pyrolysis temperature, on several samples, and the results averaged. As shown in Figure 22, the graphitization of carbon proceeded with a singularity at T_p = 1700–1800 °C (which might be related to the presence of a number of heteroatoms (e.g., O and N) in ex-PCSZ residues, even for rather high T_p values, and could modify the graphitization process).

As previously mentioned, assignment of the broad peak(s) present in the 400–1100-cm^{-1} range to silicon carbide remains uncertain, particularly at low T_p values (i.e., T_p = 1400 °C). According to a study by Sasaki et al. on ex-PCS fibers, the Raman spectrum of the 3C-polytype of SiC (the most commonly observed below 2100 °C) consists of two broad bands at 400 and 800 cm^{-1}, on one hand, and of two sharp peaks at 795 and 975 cm^{-1} (observed when the grain size becomes larger than 10 nm) on the other hand.[72] Furthermore, silica itself gives rise to a Raman spectrum with two peaks falling in the same wavenumber range, i.e., at 500 and 1100 cm^{-1}. Finally, the Raman spectrum of amorphous silicon nitride exhibited also two very broad peaks at 400 and 900 cm^{-1}.[71]

As shown in Figure 20, Raman spectra of the ex-Si–Si (Na, s) and ex-SiNME residues obtained for T_p = 1400 °C exhibit several broad peaks of significant intensity in the 400–1100-cm^{-1} range, whereas these peaks are almost nonexistent in the related ex-SiNHSi residue. Although an accurate assignment of the peaks cannot be done, as discussed above, the lack of sharp peaks at 795 and 975 cm^{-1} suggests that silicon carbide formed at this temperature remained poorly crystallized, as observed by XRD. When T_p increased, intensities of the peaks, in the 400–1100-cm^{-1} range, also increased (Figure 21). Above 1600 °C, a peak of strong intensity, but which remained rather broad, was observed at 800 cm^{-1} with a shoulder on its right-hand side at 1000 cm^{-1}. This peak could be assigned to silicon carbide.

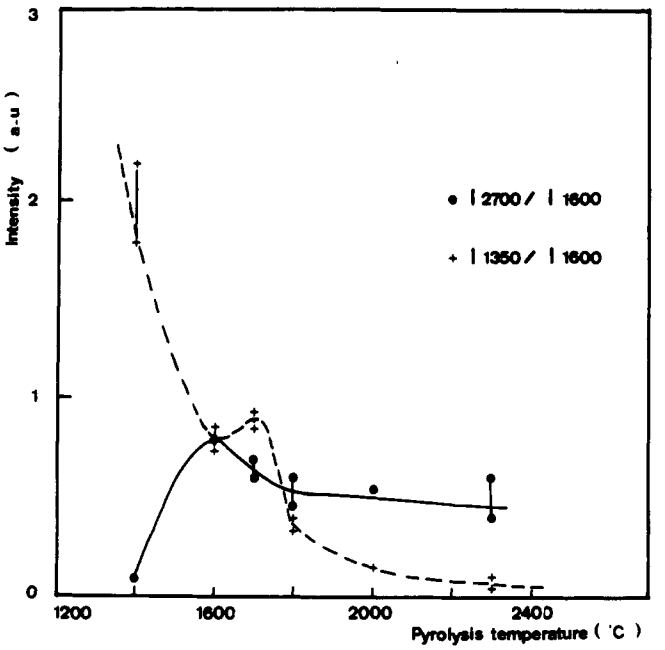

Figure 22. Evolution with T_p of the I_{2700}/I_{1600} and I_{1350}/I_{1600} ratios for the solid residues resulting from the pyrolysis of the SiNHMe precursor.

Conclusion

From the above results and discussion, the following conclusions can be drawn concerning the relations that may exist between PCS (or PCSZ) precursors and their residues of pyrolysis:

As previously suggested by Schilling et al., a PCS precursor with a *linear structure* (e.g., the Si–H model precursor) does not lead to a high amount of inorganic residue by pyrolysis under an argon pressure of 1 atm. Under these conditions, the linear polymeric chain is progressively broken into short fragments that give rise to an evolution of low boiling point species (presumably according to rearrangements involving free radicals). Therefore, such polymers must be submitted to a *cross-linking treatment* (which could be performed either thermally or chemically) before pyrolysis, to increase the ceramic yield. Such a treatment is known to be an important step in Yajima's route to ex-PCS fibers. The ceramic yield will be high when the precursor contains strong chemical bonds (e.g., Si–O bonds or Si–N bonds), which the degree of cross-linking is sufficient or, more generally speaking, when the precursor exhibits a marked ability to give rise to a three-dimensional polymeric network at the beginning of the pyrolysis (which is actually the case for the SiNHSi model precursor with respect to the other nitrogen-containing precursors studied here).

Precursors with a high percentage of organic carbon do not necessarily lead to ceramics with a high percentage of *free carbon*. As a matter of fact, the result depends strongly on the thermal stability of the hydrocarbon linkages that have been introduced into the precursor.

Introducing *nitrogen* in the organometallic precursors (PCSZ precursors) results in ceramics containing signifi-

cant percentages of nitrogen that is thought to be bonded to silicon (as Si_3N_4 or more probably as or oxycarbonitride tetrahedral species). In such ceramics, nitrogen seems to act as *an inhibitor* with respect to the recrystallization mechanisms. As a result, the ex-PCSZ ceramics are thought to keep their poorly crystallized microstructure (known to be responsible for high tensile strength in the fibrous materials) at temperatures higher than those previously reported for ex-PCS ceramics (e.g., Nicalon-type fibers).

Free carbon, in ceramics obtained by pyrolysis of PCS or PCSZ precursors at 1400 °C, has some common structural and microstructural features with carbon resulting from the pyrolysis of a phenolic resin.

Generally speaking, the main chemical bonds from the initial polymeric skeleton are not all maintained in the inorganic solid obtained by pyrolysis. As an example, the Si–Si bonds present in the various Si–Si precursors are no longer observed in the residues of pyrolysis.

The Si–O–Si chemical bridges from polysiloxane precursors give rise, after pyrolysis, to ceramics that contain silica and not silicon oxycarbide. Therefore, it is thought that silicon oxycarbide, which is present in most ex-PCS ceramics, may result from C–Si–O chemical bonds resulting from oxydation of the precursor or formed during the beginning of the organometallic–inorganic transition.[77]

Acknowledgment. We acknowledge the contribution of M. M. Delpuech and Sarthou, from CEA-CESTA, for the gas analysis of the pyrolysis products and to M. Sartre from Science of Surface, for the ESCA analyses. This work has been supported by AFME, CNRS, DRET, and SEP.

(77) Taki, T.; Okamura, K.; Sato, M. *J. Mater. Sci.* **1989**, *24*, 1263–7.